

# Scalar Direct Detection: In-Medium Effects

Graciela B. Gelmini,<sup>1,\*</sup> Volodymyr Takhistov,<sup>1,†</sup> and Edoardo Vitagliano<sup>1,‡</sup>

<sup>1</sup>*Department of Physics and Astronomy, University of California, Los Angeles  
Los Angeles, California, 90095-1547, USA*

(Dated: April 9, 2022)

A simple extension of the Standard Model consists of a scalar field that can potentially constitute the dark matter (DM). Significant attention has been devoted to probing light  $\mathcal{O}(\lesssim 10 \text{ eV})$  scalar DM, with a multitude of experimental proposals based on condensed matter systems as well as novel materials. However, the previously overlooked effective in-medium mixing of light scalars with longitudinal plasmons can strongly modify the original sensitivity calculations of the direct detection experiments. We implement the in-medium effects for scalar DM detection, using thermal field theory techniques, and show that the reach of a large class of direct DM detection experiments searching for light scalars is significantly reduced. This development identifies setups based on Dirac materials and tunable plasma haloscopes as particularly promising for scalar DM detection. Further, we also show that scalars with significant boost with respect to halo DM, such as those produced in the Sun, decay of other particles or by cosmic rays, will not suffer from in-medium suppression. Hence, multi-tonne direct DM detection experiments, such as those based on xenon or argon, also constitute a favorable target.

## I. INTRODUCTION

Unveiling the nature of dark matter (DM) remains one of the most important missions of particle physics, astrophysics and cosmology (see e.g. Ref. [1] for a review). The possible mass of the DM constituents spans an enormous range of about 19 orders of magnitude. While historically many DM searches have focused on electroweak mass scales, there has been a strong interest in recent years in exploring DM particle candidates significantly lighter than  $\mathcal{O}(\text{GeV})$ .

Additional scalar fields constitute among the simplest extensions of the SM. Light scalars can readily appear in a variety of well motivated models, e.g. as moduli [2–4], dilatons [5, 6] or in Higgs portal models [7]. The smallness of mass of a light scalar field can be attributed to an enhanced symmetry, such as a conformal symmetry or supersymmetry. In the early Universe, light scalars can be produced through the well known misalignment mechanism (e.g. [8]).

Here, we consider light scalars, which could constitute the DM and/or could be produced from some source, e.g. Sun or cosmic ray interactions, and could be detected through the energy they deposit within a detector. We remain agnostic about the particular mechanism to make the scalar we consider light, as well as to the mechanism by which it could account for the whole of the DM. In most models scalars can typically couple to fermions, and we will proceed phenomenologically and consider that the scalar field is coupled to electrons (see e.g. [7, 9–13]).

Direct detection experiments attempt to measure the energy deposited within a detector by interactions of particles passing through it. These could be DM particles in

the dark halo of our Galaxy, or particles emitted by particular sources. Halo DM particles lighter than  $\mathcal{O}(\text{GeV})$  could not deposit sufficient energy in interactions with nuclei in ton-scale direct detection experiments (e.g. [14–17]), whose energy thresholds are close to a keV. Hence, other types of searches are required to explore lighter DM particles.

Sensitivity to  $\mathcal{O}(10 \text{ eV})$  mass halo DM can be gained within large direct detection experiments searching for ionization signals due to DM absorption by bound electrons [18, 19]. Detection proposals based on materials with a small band-gap  $\mathcal{O}(\text{meV})$  envision having good sensitivity to halo DM particles with mass larger than the gap, through the efficient excitation of quasi-particles, such as phonons, magnons, and plasmons. Proposed target materials include superconductors [20, 21], graphene [22], Dirac materials [13, 23], superfluid helium [24, 25] and polar materials [26], as well as plasma haloscopes [27, 28].

In-medium effects within detectors could suppress the interactions of incoming particle and thus present a major limiting factor for experimental searches. While this is well-known for searches of dark photons, gauge vector bosons having a kinetic mixing with the SM photon [29], this effect has been ignored in the literature when discussing scalar absorption or scalar-mediated DM detection. In this work, we show that the suppression of scalar interactions in a medium can significantly modify the detection sensitivity and thus be of paramount importance in the design of experiments.

In the following, we will discuss how scalar absorption can be described with thermal field theory tools, and find that the mixing with the longitudinal plasmon affects the interaction of the scalar with the medium. We will then use superconductor detectors as an example in which in-medium effects are important. Finally, we identify possible ways to avoid the in-medium suppression that will bring us to our conclusions. The Appendices discuss the

\* gelmini@physics.ucla.edu

† vtakhist@physics.ucla.edu

‡ edoardo@physics.ucla.edu

calculation of self-energies in a plasma using thermal field theory and the absorption of scalars in superconductors.

## II. SCALAR DARK MATTER ABSORPTION

Consider a light scalar field  $\phi$  that will in general couple to the SM fermions, e.g. via a Higgs-mixing portal [7]. The resulting low energy Lagrangian is

$$\mathcal{L} \supset \frac{1}{2}(\partial_\mu \phi)^2 - \frac{1}{2}m^2 \phi^2 + \sum_f g_{\phi f} \phi \bar{f} f. \quad (1)$$

Let us assume that  $\phi$  couples to electrons through the interaction term  $g\phi\bar{e}e$  and also that it constitutes the entirety of the DM.

In a plasma,  $\phi$  can mix with the in-medium longitudinal plasmon. The latter is the quasi-particle of the longitudinal excitation of the electromagnetic field in a medium. Physically, this corresponds to a quantum of collective oscillation of the electron gas around the ions constituting the medium.

We employ thermal field theory to obtain the scalar DM absorption rate in a detector. The main advantage of resorting to this approach instead of the kinetic theory approach is that mixing effects are explicit and straightforward to implement. In the kinetic theory approach, one computes with usual quantum field theory techniques the velocity averaged absorption rate  $\langle n_e \sigma_{\text{abs}} v_{\text{rel}} \rangle$  where  $n_e$  is the electron number number density and  $\sigma_{\text{abs}}$  is the absorption cross-section. In-medium effects are included in  $\sigma_{\text{abs}}$  as “corrections” in an ad-hoc way following general arguments. Such procedure has been widely employed in the literature to treat in-medium effects in the context, for example, of dark photon absorption (e.g. [13, 18]).

Here, we follow the discussion of Refs. [28, 32] of the absorption of axions and dark photons in a detector, respectively<sup>1</sup>. The emission and absorption rates of a boson by a medium are directly related to the self-energy  $\Pi$  of the particle in the medium itself as [34, 35]

$$\text{Im } \Pi = -\omega \Gamma. \quad (2)$$

Here  $\omega$  is the particle energy and  $\Gamma = \Gamma_{\text{abs}} - \Gamma_{\text{prod}}$  is the rate with which the considered particle momentum distribution approaches thermal equilibrium. Eq. (2) is the optical theorem restated in the framework of thermal field theory. With momentum distribution  $f_\phi(\mathbf{k})$ , the scalar number density  $n$  is

$$n = \int \frac{d^3 \mathbf{k}}{(2\pi)^3} f_\phi. \quad (3)$$

For a boson with absorption rate  $\Gamma_{\text{abs}}$  and production rate  $\Gamma_{\text{prod}}$ , one finds [34]

$$\frac{\partial f}{\partial t} = -f\Gamma_{\text{abs}} + (1+f)\Gamma_{\text{prod}}. \quad (4)$$

To reduce noise, the detectors relevant for our discussion typically operate at cryogenic temperatures. Hence, we can neglect any population of photons in the medium. Plasmons are only produced by the absorption of DM. For scalar masses of  $\mathcal{O}(\lesssim 10 \text{ eV})$  the occupation number of DM bosons is large,  $f_\phi \gg 1$ , so that the scalar and photon  $A$  distributions evolve respectively as

$$\frac{\partial f_\phi}{\partial t} \simeq -f_\phi \Gamma^\phi \quad (5a)$$

$$\frac{\partial f_A}{\partial t} = -f_A \Gamma_{\text{prod}}^\phi + (1+f_A)\Gamma_{\text{abs}}^\phi, \quad (5b)$$

where  $\Gamma^\phi = \Gamma_{\text{abs}}^\phi - \Gamma_{\text{prod}}^\phi$  is the rate by which  $\phi$  particles are driven towards equilibrium.

Using  $\partial f_A / \partial t = -\partial f_\phi / \partial t$ , one has

$$\Gamma_{\text{abs}}^\phi \simeq (f_\phi - f_A)\Gamma^\phi \simeq -f_\phi \frac{\text{Im} \Pi_\phi}{\omega}, \quad (6)$$

where in the last approximation we have assumed that  $f_\phi \gg f_A$  and used Eq. (2).

At lowest order the scalar self-energy is given in the vacuum propagation basis (i.e. the mass basis) by [31]

$$\Pi_\phi = \left( \Pi^{\phi\phi} - \frac{(\Pi^{A\phi})^2}{\Pi^{AA} - m^2} \right), \quad (7)$$

where  $K = (\omega, \mathbf{k})$  is the four-momentum of the scalar, and  $\Pi^{\phi\phi}$ ,  $\Pi^{A\phi}$ , and  $\Pi^{AA}$  correspond to the forward scattering amplitudes off electrons for the processes  $\phi + e \rightarrow \phi + e$ ,  $A + e \rightarrow \phi + e$ , and  $A + e \rightarrow A + e$  respectively. The second term of Eq. (7) has long been known to be important for dark photon absorption in the detector, however its effect on scalar absorption has not been previously appreciated.

At this point, one simply needs expressions for  $\Pi^{\phi\phi}$ ,  $\Pi^{A\phi}$  and  $\Pi^{AA}$ , given in Appendix A, and substitute Eq. (7) into Eq. (6).

Using Eq. (2) and (7), and enforcing the on-shell condition  $K^2 = m_\phi^2$ , the resulting absorption rate of scalars is

$$\Gamma_{\text{abs}}^\phi = f_\phi \frac{g^2}{e^2} k^2 \omega^2 \frac{\Gamma_L}{(\omega^2 - \omega_p^2)^2 + (\omega \Gamma_L)^2}, \quad (8)$$

where  $\omega_p^2 = (\omega^2/K^2)\text{Re} \Pi_L$  is the plasma frequency (squared) and  $\Gamma_L = -Z_L \text{Im} \Pi_L / \omega$  is the damping rate of longitudinal plasmons in the material. The renormalization factor  $Z_L = \omega^2/K^2$  is needed for the longitudinal plasmon, see Appendix A. This rate closely resembles the production rate of scalars from a thermal bath of SM particles obtained in Ref. [31]. We observe that  $\omega \gg \omega_p$  and  $\omega \gg \Gamma_L$  give the relevant limit for in-medium effects to be negligible.

<sup>1</sup> The same approach has been previously used to compute the production of particles in stellar environments, see e.g. Refs. [31, 33].

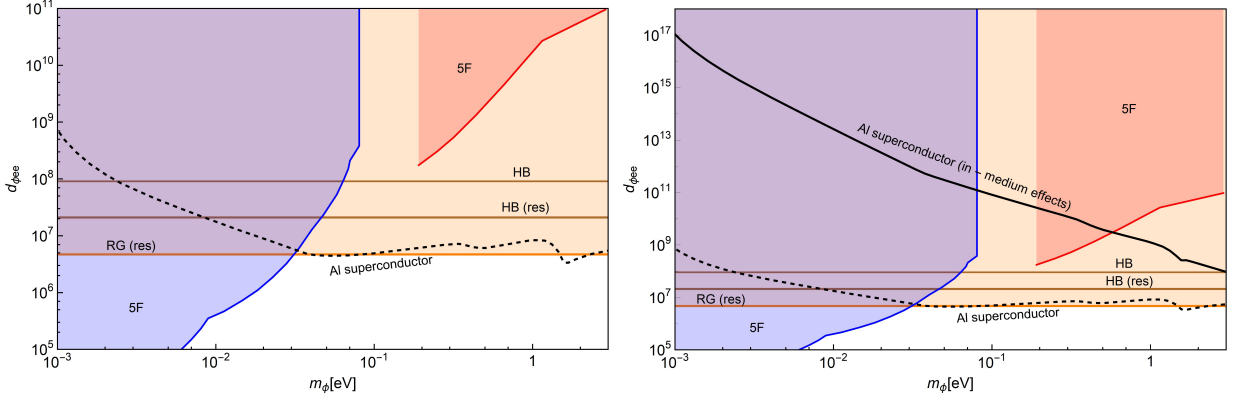


FIG. 1. Estimated sensitivity of an aluminum superconductor target for 1-kg-year exposure (left panel) without in-medium effects (dashed black) [12] and (right panel) including in-medium effects (solid black), for absorption of scalar dark matter. We also display constraints from fifth-force searches (shaded blue and red, “5F”) [30], horizontal branch cooling from continuum production (brown line, “HB”) and resonant production (thick brown line, “HB (res)”) [31], red giant resonant production (shaded orange, “RG (res)”) [31].

The above results imply that the in-medium effects can be included by defining an effective coupling of the scalar DM

$$g_{\text{eff}}^2 = g^2 \frac{m_\phi^4}{(m_\phi^2 - \omega_p^2)^2 + (m_\phi \Gamma_L)^2}, \quad (9)$$

where in the DM non-relativistic limit  $\omega \simeq m_\phi$ . We thus find that the scalar DM coupling gets modified by in-medium effects just like in the case of dark photon DM, e.g. [13, 18, 23].

### III. SCALAR ABSORPTION IN SUPERCONDUCTORS

As an example where in-medium effects are important, we consider scalar DM absorption in aluminum superconductors (see e.g. [12]). Following Ref. [12], we take the coupling of Eq. (1) to be  $g = d_{\phi ee} \sqrt{4\pi} (m_e/M_{\text{pl}})$ . The longitudinal component of the polarization tensor  $\Pi_L$  is related to the complex index of refraction  $\hat{n}$ , the complex dielectric constant  $\hat{\epsilon}$ , as well as the complex conductivity  $\hat{\sigma} = \sigma_1 + i\sigma_2$  of the medium,  $\Pi_L = K^2(1 - \hat{n}^2) = K^2(1 - \hat{\epsilon}) = -K^2(i\hat{\sigma}/\omega)$ . Using  $\sigma_1$ , the scalar absorption rate [12], including in-medium effects via coupling redefinition  $d_{\phi ee} \rightarrow d_{\phi ee, \text{eff}}$  from Eq. (9), is given by

$$R = \frac{1}{\rho_T} \frac{\rho_{\text{DM}}}{m_\phi} \frac{3}{\alpha} \left( d_{\phi ee, \text{eff}} \frac{m_e}{M_{\text{pl}}} \right)^2 \sigma_1 \times \begin{cases} \frac{5}{2} c_s^2 & , \quad \omega < \omega_D \\ \frac{5}{3} \frac{c_s^2 \omega^2}{\omega_D^2} \frac{(1 - (3\omega_D/4\omega))}{(1 - (5\omega_D/6\omega))} & , \quad \omega > \omega_D \end{cases} \quad (10)$$

where  $\rho_T$  is the mass density of target material,  $\rho_{\text{DM}} = 0.3 \text{ GeV/cm}^3$  is the local DM mass density,  $m_\phi$  is the DM mass,  $m_e$  is the electron mass,  $M_{\text{pl}}$  is the Planck mass,  $c_s \simeq 2 \times 10^{-5}$  is the sound speed in aluminum,  $\omega_D \simeq 0.037 \text{ eV}$  is the maximum frequency for phonons in aluminum and  $\sigma_1$  is the real part of the complex conductivity in aluminum, given in Ref. [12], which corresponds to the physical width  $\Gamma_L$  of the longitudinal plasmon (i.e.  $\Gamma_L = \sigma_1$  for  $\omega = m_\phi$ ).

In Fig. 1 we display the projected sensitivity for scalar DM absorption in an aluminum superconductor for 1-kg-year exposure, along with other existing bounds, comparing the cases with and without in-medium effects. The sensitivity when in-medium effects are included is suppressed with respect to the sensitivity when these effects are not included by a factor

$$\left( \frac{d_{\phi ee, \text{eff}}}{d_{\phi ee}} \right)^2 = \frac{m_\phi^4}{(m_\phi \sigma_1)^2 + (m_\phi^2 - \omega_p^2)^2}, \quad (11)$$

where  $\omega_p \simeq 12.2 \text{ eV}$  is the plasma frequency of aluminum. To treat other materials in general, one can substitute  $\omega_p^2 \rightarrow (\omega^2/K^2) \text{Re} \Pi_L$ .

### IV. MITIGATING IN-MEDIUM EFFECTS

The in-medium effects described above potentially affect the absorption of light scalar DM in a variety of materials. Besides superconductors, as in the example above, semiconductors (e.g. [22]) or polar materials [26] could also have sensitivities different than expected. In multi-tonne direct detection experiments based on xenon or argon, searches of scalar halo DM with mass of  $\mathcal{O}(\text{eV})$  focusing on an ionization signal could also be affected, in analogy to dark photon searches (e.g. [18]).

In-medium effects are negligible if one is far from resonance, i.e.  $\omega \gg \omega_p$  and  $\omega \gg \Gamma_L$ . While halo DM particles have very low characteristic speeds of  $\sim 10^{-3}$ , light scalars could be produced with much larger kinetic energies from particular sources, e.g. in the Sun [36], in cosmic ray interactions [37, 38] or in the decay of other DM particles [39]. Searches of scalars in multi-tonne xenon and argon experiments based on electron recoil energies of  $\mathcal{O}(\text{keV})$ , as e.g. in Ref. [40], are not significantly affected by in-medium effects, since  $\omega \gg \sigma_1, \sigma_2$ .

We note that in-medium effects can not only suppress a signal but also enhance it, taking advantage of the associated resonance. This is done by matching the resonance frequency with the particle mass, i.e.  $\omega_p = m_\phi$ , as accomplished with tunable plasma haloscopes [27, 28].

## V. CONCLUSIONS

We have studied here important previously ignored in-medium effects for the absorption of scalar bosons in detector materials. These effects suppress the signal of scalars in materials when their energy is not much larger than the plasma frequency  $\omega_p$  of the medium. The same effects can, on the contrary, enhance the signal through a resonant absorption in materials or metamaterials in which  $\omega_p$  can be tuned to be equal the scalar energy.

We have computed the in-medium effects for scalar detection using thermal field theory techniques, and have shown that the reach of several proposed direct detection experiments searching for light halo DM scalars is significantly weakened.

This development identifies setups, such as those based on Dirac materials and tunable plasma haloscopes, as particularly promising for scalar halo DM detection.

We have also shown that for scalars with energy much larger than  $\mathcal{O}(10 \text{ eV})$ , e.g. such as those produced in the Sun, cosmic rays or decays of other DM particles, in-medium effects are negligible. Hence, experiments searching for a keV-level ionization signal, such as those based on xenon or argon, also constitute a favorable target.

## ACKNOWLEDGMENTS

We thank G. Raffelt for discussions. The work of GG, VT and EV was supported by the U.S. Department of Energy (DOE) Grant No. DE-SC0009937.

## APPENDIX A: PARTICLE SELF-ENERGIES IN PLASMA

Here, we review the thermal field theory machinery needed to compute the self-energies of particles in a plasma. We will primarily follow the treatment of Ref. [31], where the mixing of scalars and longitudinal

plasmons has been discussed in the context of astrophysical environments. This approach is well known and has been previously applied to the production of other particles in stars, like dark photons (e.g. [33, 41]) and neutrinos (e.g. [42, 43]). In-medium interactions can be accounted for by including a linear response (see, for instance, Refs. [43, 44]),

$$J_{\text{ind}}^\mu = -\Pi^{\mu\nu} A_\nu, \quad (12)$$

where  $\Pi^{\mu\nu}$  is a polarization tensor. Hence, the total current coupling to photon is  $eJ_{\text{EM}}^\mu + J_{\text{ind}}^\mu$ .

In the Lorentz gauge, the polarization tensor is described by two polarization functions  $\Pi_T$  and  $\Pi_L$ , for transverse and longitudinal excitations (e.g. [18])

$$\begin{aligned} \Pi^{\mu\nu} &\equiv ie^2 \langle J_{\text{EM}}^\mu J_{\text{EM}}^\nu \rangle = -\Pi_T (e_+^\mu e_+^{*\nu} + e_-^\mu e_-^{*\nu}) - \Pi_L e_L^\mu e_L^{*\nu} \\ &= \sum_{i=\pm, L} \Pi_i P_i^{\mu\nu}, \end{aligned} \quad (13)$$

where  $e_L$  and  $e_{+,-}$  are the longitudinal and the transverse polarization vectors and  $P_i^{\mu\nu}$  are projectors. Assuming  $\mathbf{k}$  parallel to the  $\hat{z}$  axis, the polarization vectors are

$$e_L \equiv \frac{(k^2, \omega \mathbf{k})}{k\sqrt{K^2}} \quad \text{and} \quad e_{+,-} \equiv \frac{1}{\sqrt{2}}(0, \mathbf{e}_x \pm i\mathbf{e}_y), \quad (14)$$

where  $\mathbf{e}_x, \mathbf{e}_y$  are orthogonal unit vectors perpendicular to the unit vector  $\mathbf{k}/k$ .

To lowest order, the real part of the polarization tensor is directly taken from the forward scattering on charged particles. Moreover, because the scattering amplitude involves for a non-relativistic plasma the inverse mass of the targets, we can limit our attention to electrons. Thus, the real part of the polarization tensor is

$$\begin{aligned} \text{Re } \Pi^{\mu\nu}(K) &= 4e^2 \int \frac{d^3p}{(2\pi)^3} \frac{1}{2E_p} (f_e(E_p) + f_{\bar{e}}(E_p)) \\ &\times \frac{P \cdot K (P^\mu K^\mu + K^\mu P^\mu) - K^2 P^\mu P^\nu - (P \cdot K)^2 g^{\mu\nu}}{(P \cdot K)^2 - (K^2)^2/4}, \end{aligned} \quad (15)$$

which is correct to order  $\alpha$ . Here,  $f_e$  and  $f_{\bar{e}}$  are the distribution functions for electrons and positrons. In the non-relativistic limit, one considers only electrons. As discussed in Refs. [42, 44], the  $K^4$  term in the denominator can be neglected.

Ignoring the  $K^4$  term and multiplying by the projectors, in the lowest order of electron velocities one obtains [33, 44]

$$\text{Re } \Pi_T = \omega_p^2, \quad (16a)$$

$$\text{Re } \Pi_L = \frac{K^2}{\omega^2} \omega_p^2. \quad (16b)$$

The dispersion relation for the transverse plasmon is  $\omega^2 - k^2 = \omega_p^2$ . This allows for an interpretation of transverse excitations as particles with mass  $\omega_p$ . In a plasma we have  $\omega_p = e^2 n_e / m_e$ , while in a metal one

has to use the effective mass of electrons  $m_e^*$ . Longitudinal plasmons instead have a dispersion relation given by  $\omega^2 = \omega_p^2$ .

The imaginary part of the polarization tensor can be potentially computed via Kramers-Kronig relations, or experimentally measured. The transverse plasmon absorption is given for a non-relativistic plasma by  $\Gamma_T = -\text{Im} \Pi_L / \omega$ . When treating longitudinal plasmons one defines the vertex renormalization constant  $Z_L = \omega^2 / K^2$ , which must be included for external longitudinal plasmon in a diagram. In this way, the longitudinal rate is  $\Gamma_L = -Z_L \text{Im} \Pi_L / \omega$ .

We can now turn our focus on the scalar self-energy computation. The one-loop electron self-energies, assuming the Lagrangian of Eq. (1), are

$$\begin{aligned} \text{Re} \Pi_{\phi A}^\mu(K) &= 4g_\phi e \int \frac{d^3 p}{(2\pi)^3} \frac{1}{2E_p} (f_e(E_p) + f_{\bar{e}}(E_p)) \\ &\times m_e \frac{(P \cdot K) K^\mu - K^2 P^\mu}{(P \cdot K)^2 - (K^2)^2/4}, \end{aligned} \quad (17)$$

for the scalar-scalar mixing and

$$\begin{aligned} \text{Re} \Pi^{\phi\phi}(K) &= 4g_\phi^2 \int \frac{d^3 p}{(2\pi)^3} \frac{1}{2E_p} (f_e(E_p) + f_{\bar{e}}(E_p)) \\ &\times \frac{(P \cdot K)^2 - m_e^2 K^2}{(P \cdot K)^2 - (K^2)^2/4}, \end{aligned} \quad (18)$$

for the scalar-photon mixing. In a non-relativistic plasma, this gives

$$\text{Re} \Pi^{\phi L} = \text{Re} \Pi_{\phi A}^\mu e_\mu^L \simeq g e \frac{k \sqrt{K^2}}{\omega^2} \frac{n_e}{m_e}. \quad (19)$$

At lowest order the scalar self-energy is given by [31]

$$\Pi_\phi = \left( \Pi^{\phi\phi} - \frac{(\Pi^{A\phi})^2}{\Pi^{AA} - m^2} \right), \quad (20)$$

where  $K = (\omega, \mathbf{k})$  is the four-momentum of the external scalar, and  $\Pi^{\phi\phi}$ ,  $\Pi^{A\phi}$ , and  $\Pi^{AA}$  correspond to the forward scattering amplitudes over electrons for the processes  $\phi + e \rightarrow \phi + e$ ,  $A + e \rightarrow \phi + e$ , and  $A + e \rightarrow A + e$  respectively. One then finds

$$\begin{aligned} \text{Im} \Pi^\phi &= \text{Im} \Pi^{\phi\phi} \\ &+ \frac{\text{Im} \Pi^{AA} ((\text{Re} \Pi^{A\phi})^2 - (\text{Im} \Pi^{A\phi})^2)}{(\text{Im} \Pi^{AA})^2 + (\text{Re} \Pi^{AA} - m^2)^2} \\ &- \frac{2(\text{Re} \Pi^{AA} - m^2) \text{Re} \Pi^{A\phi} \text{Im} \Pi^{A\phi}}{(\text{Im} \Pi^{AA})^2 + (\text{Re} \Pi^{AA} - m^2)^2}. \end{aligned} \quad (21)$$

Enforcing the on-shell condition  $K^2 = m_\phi^2$ , the resulting absorption rate of scalars is (see also Ref. [31])

$$\Gamma_{\text{abs}}^\phi = f_\phi \frac{g^2}{e^2} k^2 \omega^2 \frac{\Gamma_L}{(\omega^2 - \omega_p^2)^2 + (\omega \Gamma_L)^2}. \quad (22)$$

The absorption rate of scalars per unit mass from a detector is thus

$$\begin{aligned} R &= \frac{1}{\rho_T} \int \frac{d^3 \mathbf{k}}{(2\pi)^3} \Gamma_{\text{abs}}^\phi \\ &= \frac{1}{\rho_T} \int \frac{d^3 \mathbf{k}}{(2\pi)^3} f_\phi \frac{g^2}{e^2} k^2 m^2 \frac{\Gamma_L}{(m^2 - \omega_p^2)^2 + (m \Gamma_L)^2}, \end{aligned} \quad (23)$$

where  $\rho_T$  is the detector mass density.

## APPENDIX B: ABSORPTION IN SUPERCONDUCTORS

We summarize below the treatment of scalar absorption rate in superconductors following Ref. [12]. The problem can be described in terms of macroscopic quantities and the results matched into particle physics model parameters via Feynman diagram calculation. The general DM-electron absorption rate is given by

$$\begin{aligned} R &= \frac{1}{\rho_T} \int \frac{d^3 \mathbf{k}}{(2\pi)^3} \Gamma_{\text{abs}}^\phi \\ &= \frac{1}{\rho_T} \frac{\rho_{\text{DM}}}{m_{\text{DM}}} \langle n_e \sigma_{\text{abs}} v_{\text{rel}} \rangle \end{aligned} \quad (24)$$

where,  $\sigma_{\text{abs}}$  is the absorption cross-section,  $n_e$  is the electron number density and the average is over DM velocity  $v_{\text{rel}}$ . The DM absorption rate can be directly related to the photon absorption rate specified via  $\langle n_e \sigma_{\text{abs}} v_{\text{rel}} \rangle_\gamma$ , which has been experimentally measured.

In the limit of small momentum transfer  $q \ll \omega$  compared to energy  $\omega$ , transverse and longitudinal parts of polarization tensor characterizing the medium are equal and are related to the complex conductivity as

$$\Pi(\omega) \simeq \Pi_T(\omega) \simeq \Pi_L(\omega) \simeq -i\hat{\sigma}\omega. \quad (25)$$

From optical theorem, photon absorption rate can be related to the polarization tensor via

$$\langle n_e \sigma_{\text{abs}} v_{\text{rel}} \rangle_\gamma = -\frac{\text{Im} \Pi(\omega)}{\omega}. \quad (26)$$

The absorption is characterized by  $\sigma_1$ , with  $\sigma_1 = \langle n_e \sigma_{\text{abs}} v_{\text{rel}} \rangle_\gamma$ .

Using standard Drude model for metals to description the conductivity, one obtains

$$\sigma_1(\omega) \simeq \frac{\omega_p^2}{\omega^2 \tau}, \quad \sigma_2(\omega) \simeq \frac{\omega_p^2}{\omega}, \quad (27)$$

where  $\omega_p \simeq 12.2$  eV is the plasma frequency in aluminum and  $\tau$  represents electron scattering time in a medium. In the above  $\omega\tau \gg 1$  has been assumed and also that  $\tau$  does not depend on temperature, envisioning a cryogenic system.

Here, the interaction time  $\tau$  is set by athermal phonons interacting with electrons. Using Debye model for



phonon dispersion, one obtains

$$\frac{1}{\tau} = \begin{cases} \frac{4}{5}\pi\lambda_{\text{tr}}\omega_D(1 - \frac{5}{6}\frac{\omega_D}{\omega}) & , \omega \geq \omega_D \\ \frac{2}{15}\pi\lambda_{\text{tr}}\frac{\omega^5}{\omega_D^4} & , \omega < \omega_D \end{cases} \quad (28)$$

where for aluminum  $\omega_D \simeq 0.037$  eV and the measured high temperature resistivity is  $\lambda_{\text{tr}} = 0.39$  [45].

While the Drude model is in general only valid for met-

als in a non-superconducting phase, the difference appears when one is close to the superconducting gap  $2\Delta$  and can be accommodated as in Ref. [46] via modification of time  $\tau/\tau_{\text{super}} = f(\Delta)$  where  $f(\Delta)$  is a integral function of the gap. This will only start to affect the results when  $\omega \lesssim 10^{-2}$  [12].

Matching the matrix elements  $|\mathcal{M}|^2 \propto |\mathcal{M}_\gamma|^2$  for scalar and photon interactions and using the above obtained macroscopic quantities, one obtains the absorption rate for scalars as described in Eq. (10). For our approximate results in the manuscript, we employ the  $\sigma_1$  obtained in Ref. [12] for normal metals (see their Fig. 2).

- 
- [1] G. B. Gelmini, *The Hunt for Dark Matter*, in *TASI: Journeys Through the Precision Frontier: Amplitudes for Colliders*, pp. 559–616, 2015, [1502.01320](#), DOI.
  - [2] C. Burgess, A. Maharana and F. Quevedo, *Über-naturalness: unexpectedly light scalars from supersymmetric extra dimensions*, *JHEP* **05** (2011) 010 [[1005.1199](#)].
  - [3] M. Cicoli, C. Burgess and F. Quevedo, *Anisotropic Modulus Stabilisation: Strings at LHC Scales with Micron-sized Extra Dimensions*, *JHEP* **10** (2011) 119 [[1105.2107](#)].
  - [4] S. Dimopoulos and G. Giudice, *Macroscopic forces from supersymmetry*, *Phys. Lett. B* **379** (1996) 105 [[hep-ph/9602350](#)].
  - [5] T. Damour and A. M. Polyakov, *The String dilaton and a least coupling principle*, *Nucl. Phys. B* **423** (1994) 532 [[hep-th/9401069](#)].
  - [6] T. Taylor and G. Veneziano, *Dilaton Couplings at Large Distances*, *Phys. Lett. B* **213** (1988) 450.
  - [7] F. Piazza and M. Pospelov, *Sub-eV scalar dark matter through the super-renormalizable Higgs portal*, *Phys. Rev. D* **82** (2010) 043533 [[1003.2313](#)].
  - [8] P. Arias, D. Cadamuro, M. Goodsell, J. Jaeckel, J. Redondo and A. Ringwald, *WISPy Cold Dark Matter*, *JCAP* **06** (2012) 013 [[1201.5902](#)].
  - [9] E. Adelberger, B. Heckel and A. Nelson, *Tests of the gravitational inverse-square law*, *Annual Review of Nuclear and Particle Science* **53** (2003) 77–121.
  - [10] A. Arvanitaki, J. Huang and K. Van Tilburg, *Searching for dilaton dark matter with atomic clocks*, *Physical Review D* **91** (2015) .
  - [11] A. Arvanitaki, S. Dimopoulos and K. Van Tilburg, *Sound of dark matter: Searching for light scalars with resonant-mass detectors*, *Physical Review Letters* **116** (2016) .
  - [12] Y. Hochberg, T. Lin and K. M. Zurek, *Detecting Ultralight Bosonic Dark Matter via Absorption in Superconductors*, *Phys. Rev. D* **94** (2016) 015019 [[1604.06800](#)].
  - [13] Y. Hochberg, Y. Kahn, M. Lisanti, K. M. Zurek, A. G. Grushin, R. Ilan, S. M. Griffin, Z.-F. Liu, S. F. Weber and J. B. Neaton, *Detection of sub-MeV Dark Matter with Three-Dimensional Dirac Materials*, *Phys. Rev. D* **97** (2018) 015004 [[1708.08929](#)].
  - [14] E. Aprile, J. Aalbers, F. Agostini, M. Alfonsi, L. Althueser, F. Amaro, V. Antochi, E. Angelino, F. Arneodo, D. Barge and et al., *Search for light dark matter interactions enhanced by the migdal effect or bremsstrahlung in xenon1t*, *Physical Review Letters* **123** (2019) .
  - [15] XENON Collaboration, E. Aprile et al., *Constraining the spin-dependent WIMP-nucleon cross sections with XENON1T*, *Phys. Rev. Lett.* **122** (2019) 141301 [[1902.03234](#)].
  - [16] DARKSIDE Collaboration, P. Agnes et al., *Constraints on Sub-GeV Dark-Matter–Electron Scattering from the DarkSide-50 Experiment*, *Phys. Rev. Lett.* **121** (2018) 111303 [[1802.06998](#)].
  - [17] LUX Collaboration, D. Akerib et al., *Results from a search for dark matter in the complete LUX exposure*, *Phys. Rev. Lett.* **118** (2017) 021303 [[1608.07648](#)].
  - [18] H. An, M. Pospelov, J. Pradler and A. Ritz, *Direct Detection Constraints on Dark Photon Dark Matter*, *Phys. Lett. B* **747** (2015) 331 [[1412.8378](#)].
  - [19] I. M. Bloch, R. Essig, K. Tobioka, T. Volansky and T.-T. Yu, *Searching for Dark Absorption with Direct Detection Experiments*, *JHEP* **06** (2017) 087 [[1608.02123](#)].
  - [20] Y. Hochberg, Y. Zhao and K. M. Zurek, *Superconducting Detectors for Superlight Dark Matter*, *Phys. Rev. Lett.* **116** (2016) 011301 [[1504.07237](#)].
  - [21] Y. Hochberg, M. Pyle, Y. Zhao and K. M. Zurek, *Detecting Superlight Dark Matter with Fermi-Degenerate Materials*, *JHEP* **08** (2016) 057 [[1512.04533](#)].
  - [22] Y. Hochberg, Y. Kahn, M. Lisanti, C. G. Tully and K. M. Zurek, *Directional detection of dark matter with two-dimensional targets*, *Phys. Lett. B* **772** (2017) 239 [[1606.08849](#)].
  - [23] A. Coskuner, A. Mitridate, A. Olivares and K. M. Zurek, *Directional Dark Matter Detection in Anisotropic Dirac Materials*, [1909.09170](#).
  - [24] S. Knapen, T. Lin and K. M. Zurek, *Light Dark Matter in Superfluid Helium: Detection with Multi-excitation Production*, *Phys. Rev. D* **95** (2017) 056019 [[1611.06228](#)].
  - [25] K. Schutz and K. M. Zurek, *Detectability of Light Dark Matter with Superfluid Helium*, *Phys. Rev. Lett.* **117** (2016) 121302 [[1604.08206](#)].
  - [26] S. Knapen, T. Lin, M. Pyle and K. M. Zurek, *Detection of Light Dark Matter With Optical Phonons in Polar Materials*, *Phys. Lett. B* **785** (2018) 386 [[1712.06598](#)].
  - [27] M. Lawson, A. J. Millar, M. Pancaldi, E. Vitagliano

- and F. Wilczek, *Tunable axion plasma haloscopes*, *Phys. Rev. Lett.* **123** (2019) 141802 [[1904.11872](#)].
- [28] G. B. Gelmini, A. J. Millar, V. Takhistov and E. Vitagliano, *Probing Dark Photons with Plasma Haloscopes*, [2006.06836](#).
- [29] B. Holdom, *Two  $U(1)$ 's and Epsilon Charge Shifts*, *Phys. Lett. B* **166** (1986) 196.
- [30] E. Adelberger, B. R. Heckel and A. Nelson, *Tests of the gravitational inverse square law*, *Ann. Rev. Nucl. Part. Sci.* **53** (2003) 77 [[hep-ph/0307284](#)].
- [31] E. Hardy and R. Lasenby, *Stellar cooling bounds on new light particles: plasma mixing effects*, *JHEP* **02** (2017) 033 [[1611.05852](#)].
- [32] A. Caputo, A. J. Millar and E. Vitagliano, *Revisiting longitudinal plasmon-axion conversion in external magnetic fields*, [2005.00078](#).
- [33] J. Redondo and G. Raffelt, *Solar constraints on hidden photons re-visited*, *JCAP* **08** (2013) 034 [[1305.2920](#)].
- [34] H. A. Weldon, *Simple rules for discontinuities in finite temperature field theory*, *Phys. Rev. D* **28** (1983) 2007.
- [35] J. Kapusta and C. Gale, *Finite-temperature field theory: principles and applications*, Cambridge Monographs on Mathematical Physics. Cambridge University Press, 2011, [10.1017/CBO9780511535130](#).
- [36] R. Budnik, O. Davidi, H. Kim, G. Perez and N. Priel, *Searching for a solar relaxion or scalar particle with XENON1T and LUX*, *Phys. Rev. D* **100** (2019) 095021 [[1909.02568](#)].
- [37] T. Bringmann and M. Pospelov, *Novel direct detection constraints on light dark matter*, *Phys. Rev. Lett.* **122** (2019) 171801 [[1810.10543](#)].
- [38] R. Plestid, V. Takhistov, Y.-D. Tsai, T. Bringmann, A. Kusenko and M. Pospelov, *New Constraints on Millicharged Particles from Cosmic-ray Production*, [2002.11732](#).
- [39] K. Agashe, Y. Cui, L. Necib and J. Thaler, *(In)direct Detection of Boosted Dark Matter*, *JCAP* **10** (2014) 062 [[1405.7370](#)].
- [40] XENON Collaboration, E. Aprile et al., *Observation of Excess Electronic Recoil Events in XENON1T*, [2006.09721](#).
- [41] H. An, M. Pospelov and J. Pradler, *New stellar constraints on dark photons*, *Phys. Lett. B* **725** (2013) 190 [[1302.3884](#)].
- [42] E. Braaten and D. Segel, *Neutrino energy loss from the plasma process at all temperatures and densities*, *Phys. Rev. D* **48** (1993) 1478 [[hep-ph/9302213](#)].
- [43] M. Haft, G. Raffelt and A. Weiss, *Standard and nonstandard plasma neutrino emission revisited*, *Astrophys. J.* **425** (1994) 222 [[astro-ph/9309014](#)]. [Erratum: *Astrophys.J.* 438, 1017 (1995)].
- [44] G. G. Raffelt, *Stars as laboratories for fundamental physics*. Chicago, USA: Univ. Pr., 1996.
- [45] P. B. Allen, *Empirical electron-phonon  $\lambda$  values from resistivity of cubic metallic elements*, *Phys. Rev. B* **36** (1987) 2920.
- [46] P. B. Allen, *Electron-phonon effects in the infrared properties of metals*, *Phys. Rev. B* **3** (1971) 305.